Scien. Tech. Bull-Chem. Food Sci. Eng., Vol. 18(XIX), 2021, 10-17

ARTICLE

FT-IR CHARACTERIZATION OF CELLULOSE CRYSTALLINITY FROM RAW BAST FIBERS

Dorina Rodica CHAMBRE[1], **Mihaela DOCHIA**[2*]

[1]Faculty of Food Engineering, Tourism and Environmental Protection, "Aurel Vlaicu" University, Romania, 2 Elena Dragoi, Arad 310330, Romania
[2]Research Development Innovation in Natural and Technical Sciences Institute, "Aurel Vlaicu" University, Romania, 2 Elena Dragoi, Arad 310330, Romania
Corresponding author email: dochiamihaela@yahoo.com

Abstract: *This paper presents the characterization of native cellulose from the jute, hemp, and flax raw fibers by infrared evaluation of crystallinity ratio (Total Crystallinity Index and Lateral Order Index) and Hydrogen Bond Intensity. The results showed that cellulose from jute fiber has a higher degree of crystallinity while that of hemp fibers has a more ordered structure, with more cellulose chains in a highly organized form. In the flax fibers, the cellulose chains are composed of a larger number of amorphous domains. Hydrogen bond intensity values were influenced by both the ordered cellulose structure and the lignin content of the fibers.*

Keywords: bast fibers, native cellulose, infrared crystallinity, hydrogen bond intensity

INTRODUCTION

The intense development of the synthetic polymer industry in recent years has led to several problems related to the large amount of non-degradable residues accumulated in the environment which have become pollutants in soil and water. This has led to the reconsideration of natural polymers which have become a sustainable and non-polluting alternative in various fields (Mustata et al., 2015).

The lignocellulosic fibers such as hemp, jute, and flax (bast fibers), due to their physicochemical properties and mechanical characteristics, are increasingly used as substitutes for synthetic compounds in various industrial fields. For instance, in the textile industry, the bast fibers are used to obtain a wide range of products, while in the field of automotive or construction materials, they are used as reinforcing agents to obtain biocomposites (Chambre and Dochia, 2020.; Donatelli et al., 2017; Karus and Kaup, 2002; Ouajai and Shanks, 2005). Obtaining quality end-products based on lignocellulosic components is influenced both by the chemical composition of the bast fibers and by the arrangement of the cellulose chains concerning each other (crystallinity) and to the fiber axis (Mustata et al., 2015).

In the chemical composition of bast fibers along with cellulose, which is the major component, there are also some non-cellulosic attendants such as pectin, lignin, hemicelluloses, waxes, etc. which influence the properties and behavior during fibers treatments (Abdel-Halim et al., 2008; Chambre et al., 2019; Ciolacu et al., 2011). While the cellulose consists of crystalline and amorphous domains, in variable proportions (depending on both source and plant variety) the non-cellulosic attendants are amorphous structures. The reactants can penetrate only the amorphous regions with a low ordered structure of cellulosic chains and it is only in these regions and on the surface of the crystallites that the reactions can take place, leaving the crystalline regions unaffected (Ciolacu et al., 2011). Under these conditions, a rigorous evaluation of the crystallinity degree of cellulosic and lignocellulosic materials becomes necessary to obtain quality end-products.

X-ray diffraction (XRD) technique was frequently used to characterize the supramolecular structure of cellulose from fibers and to reveal the modifications that occur after the dissolution/regeneration of cellulose processes (Ciolacu et al., 2011; Eichhorn et al., 2001; Mewoli et al., 2020; Ouajai and Shanks, 2005; Shahzad, 2012).

Nowadays, Fourier Transform Infrared spectroscopy (FTIR) has become a powerful analytical technique to characterize both the changes that occur in the chemical composition of natural textile fibers subjected to various treatments and their crystallinity (Chambre and Dochia, 2018.; Chambre et al., 2019; Ciolacu et al., 2011; Fan et al., 2012; O'Connor et al., 1958; Ouajai and Shanks, 2005). Based on the absorbance values of specific bands, both the crystallinity ratio and the intensity of the hydrogen bonds can be evaluated from the FTIR spectra (Fan et al., 2012; Poletto et al., 2014).

This paper aims to characterize by FTIR ATR spectroscopy some raw bast fibers (hemp, flax, and jute) as well to evaluate the infrared crystallinity ratio through determination of *Lateral Order Index, Total Crystallinity Index,* and *Hydrogen Bond Intensity* values.

MATERIALS AND METHODS

Materials

Raw jute (*Corchorus olitorius*), hemp (*Cannabis sativa*), and flax (*Linum hirsutum*) fibers were taken in the analysis. The jute fibers samples (specific mass: 1.44g/cm^3; the average length of elementary fibers: 5mm; average thickness: 18 µm; fineness: 4000 Nm) were purchased from a twine manufacturer in Bucharest. The hemp fiber samples (specific mass: 1.48 g/cm^3; the average length of elementary fibers: 22 mm; average thickness: 20 µm; fineness: 4000 Nm) were purchased from a cultivator in north-eastern Romania, while the flax fibers samples (specific mass: 1.50g/cm^3; the average length of elementary fibers: 30 mm; the average thickness: 15 µm; fineness: 6000 Nm) were obtained from a fibers processor in Fălticeni. Both flax and jute raw fibers were imported from Asia. Before analysis, the raw fibers were carefully cleaned of mechanical impurities and then conditioned on Sartorius MA 100 system at 105^0 C to constant mass. For FT-IR analyzes, the fibers samples were finely chopped.

Method

The FT-IR spectra of the fibers were acquired with a Vertex 70 (Bruker, Germany) spectrophotometer equipped with a Pike Miracle ATR cell. The spectral data were recorded on the 600-4000 cm^{-1} wavelength range with a resolution of 4 cm^{-1}. A total of 64 scans were taken for each sample. The OPUS 6.5 (Bruker) software was used both for the acquisition and processing of spectra and for the extraction of average spectra of each fiber type. Before each measurement, the ZnSe crystal (fixed at an incidence angle of 45^0) of the single reflection horizontal ATR accessory was carefully cleaned with isopropyl alcohol and the background was collected. For each fiber type, the FT-IR ATR measurements were performed in triplicate. The absorbance values (*A*) for the interest bands were evaluated from the vector normalized spectra at the 1314 cm^{-1} band which is assigned to CH$_2$ rocking vibration.

The *infrared crystallinity ratio* was determined by the following methods:

- *Lateral Order Index (LOI)*

$$LOI = \frac{A_{1424}}{A_{897}} \qquad \text{(Eq.1.)}$$

were: A_{1242} is the absorbance value of the band located at ~1424 cm^{-1}; A_{897} is the absorbance value of the band located at ~897 cm^{-1}

- *Total Crystallinity Index (TCI)*

$$TCI = \frac{A_{1367}}{A_{2920}} \qquad \text{(Eq.2.)}$$

were: A_{1368} is the absorbance value of the band located at ~1367 cm^{-1}; A_{2920} is the absorbance value of the band located at ~2920 cm^{-1}

The *Hydrogen Bond Intensity (HBI)* by (Eq.3.):

$$HBI = \frac{A_{3337}}{A_{1317}} \qquad \text{(Eq.3.)}$$

were: A_{3334} is the absorbance value of the band located at ~3337 cm^{-1}; A_{1348} is the absorbance value of the band located at ~1317 cm^{-1}

RESULTS AND DISCUSSIONS

Hemp, flax, and jute fibers are lingo-cellulosic materials (bast fibers) that are extracted from the stems of plants with the same name. The bast fibers are multicellular and have all the cells with the same structure. The differences between them refer to the external shape, to the dimensions, to the proportion between the chemical components, and some structural details. The chemical composition (wt% - the percentage of total weight) of the jute, hemp, and flax fibers reported in the literature is shown in Table 1.

Table 1. Chemical composition of the bast fibers used in the study

Fibers	Cellulose (wt%)	Hemicelluloses (wt%)	Lignin (wt%)	Pectin (wt%)	Waxes and extractable substances (wt%)	Ref.
Jute	45 - 71	13 - 20	12 - 26	0.2 - 10	0.5 - 2.5	(Poletto et al., 2014; Summerscales et al., 2010)
Hemp	74 - 77	14 - 21	3.7 - 5.5	0.9- 1.55	4 - 5	(Chambre and Dochia, 2018.; Manaia et al., 2019; Shahzad, 2012; Väisänen et al., 2018)
Flax	71 - 76	17 - 28	2.2 - 7.0	2 - 5	6.5 – 9.5	(Abdel-Halim et al., 2008; Chambre and Dochia, 2020.; Summerscales et al., 2010)

From Table 1 it can be noticed that cellulose, hemicelluloses, and lignin are the main components that have an important influence on the chemical, mechanical, physical, and end-use properties of the bast fibers (Poletto et al., 2014; Shamolina et al., 2003). The crystallinity properties of the fibers may be affected by the high content of non-cellulosic attendants which, as is known, have a pronounced amorphous character. In addition, waxes and pectin are responsible for the non-wetting the behaviour of cellulosic and lingo-cellulosic fibers by water, causing several technical problems during the dyeing and finishing processes (Chambre et al., 2019; Choe et al., 2018; Dochia et al., 2018).

Figure 1 presents the FT-IR ATR normalized average spectra (average of three recorded spectra for each type of fibers) of the jute, hemp, and flax raw fibers recorded on 600 - 4000 cm^{-1}.

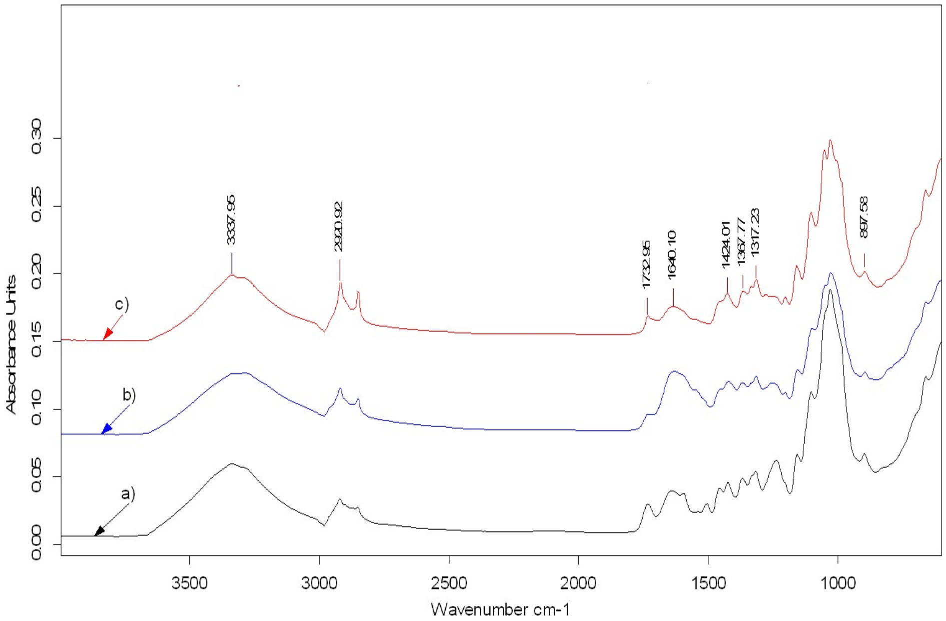

Figure 1. FT-IR ATR normalized average spectrum of the bast fibers: a) jute; b) hemp; c) flax

The "fingerprint area" is located between 600 cm^{-1} and 1500 cm^{-1} and contains specific and common bands (Dai and Fan, 2010; Rémy Legrand et al., 2020) of fibers constituents.

The main infrared vibrations as well as the assigned functional groups are presented in Table 2.

Table 2. FT-IR absorbance bands (frequency number, cm^{-1}) of main constituents from investigated raw fibers

Assigned functional groups (vibration)				Frequency number (cm^{-1})			Ref.
Cellulose	Hemicellulose	Lignin	Pectin	Jute fibers	Hemp fibers	Flax fibers	
OH stretching vibration; the intramolecular hydrogen bond of O(3)H--O(5), O(2)—O(6) intermolecular hydrogen bond of O(6)H—O(3) in cellulose I				3337 3285	3334 3287	3337 3288	(Bakri and Jayamani, 2016; Ciolacu et al., 2011; Dai and Fan, 2010; Donatelli et al., 2017; Mustata et al., 2015; Shamolina et al., 2003)
C-H symmetrical stretching (2900 cm^{-1})	C-H symmetrical stretching	C-H stretching in aromatic methoxyl group and methylene group	C-H symmetrical stretching	2921	2918	2920	
	CH_2 asymmetric stretching	CH_2 asymmetric stretching	CH_2 asymmetric stretching	2850	2851	2849	
	Stretching vibration of acetyl and uronic ester groups attached to hemicelluloses (1740 cm^{-1})	Conjugate C=O groups of hydroxycinnamic acids	C=O stretching from carboxyl and ester groups of polygalacturonic acid	1732	1730	1731	
	O-H bending vibration principally related to the presence of water in hemicellulose		Symmetric and asymmetric stretching of COO^- from Ca^{2+} pectate	1642	1639	1640	
		C=C aromatic symmetrical stretching and polyphenolic groups vibrations		1595 1505	-	-	
HCH bending of crystalline cellulose	C-H bending and OCH in plane bending vibration			1424	1424	1425	
C-OH in plane bending				1367	1367	1366	
CH_2 rocking vibration at C6 in cellulose I and cellulose II				1317	1316	1317	
		C-O, C-C, C=O and G ring stretching in lignin		1248	1245	1246	
C-O-C symmetric stretching of cellulose, O-H plane deformation	C-O-C symmetric stretching of hemicellulose			-	1203	1202	
Asymmetrical bending of C-O-C group of amorphous cellulose				1157	1156	1159	
	C-O and C-C stretching band of xylanes and C-O-C stretching of the glycosidic linkage			1054	1054	1057	
	Aromatic C-H in plane deformation and C-O stretching	Aromatic C-H in plane deformation and C-O stretching of lignin		1030	1038	1029	
C-H bending of amorphous cellulose				897.	896.	897	
C-C-O, C-O-C stretching of β-(1→4)- glycosidic linkages							
C-OH out-of-plane bending				661	660	661	

The wide bands observed at ~ 3337 cm^{-1} and ~ 3287 cm^{-1} can be correlated with the stretching vibration of groups (OH) in polysaccharides (Donatelli et al., 2017; Poletto et al., 2014) . The (OH) groups can be associated, by hydrogen bonds, both intra-, and inter-molecular as well as with adsorbed water molecules. In cellulose, the hydrogen bond associations are distributed both in crystalline and amorphous domains and it is possible to establish a relation between the OH-bands and the cellulose structure (Fan et al., 2012). According to the Gardner-Blackwell model, reported in the literature by some authors (Fan et al., 2012), hydrogen bonds for cellulose I include two intra-molecular bonding (O(2)H---O(6) and O(3)---O(5)) and one inter-molecular bonding (O(6)---O(3)) recorded between 3350 cm^{-1} and 3230 cm^{-1}.

The bands recorded at ~2920 cm^{-1} and ~ 2850 cm^{-1} can be associated with the (C-H) and (CH_2) symmetric and asymmetric stretching vibration from fibers components (Rémy Legrand et al., 2020). The literature mentions that the stretching vibration of (CH) for cellulose occurs at 2900 cm^{-1} and the presence of amorphous non-cellulosic attendants leads to the recording of two extra intense bands, one shifted to a higher value of wavenumber and the other one to a smaller value.(Chambre and Dochia, 2020.; Ciolacu et al., 2011; Rémy Legrand et al., 2020; Shamolina et al., 2003). So, for the investigated bast fibers the two bands recorded on 3000-2800 cm^{-1} range can be associated with the presence of pectin, waxes, and hemicelluloses. According to Table 1 data, the intense bands observed in the spectra of flax fibers at ~ 2920 cm^{-1} and ~ 2850 cm^{-1} are due to the presence of a higher content of pectin and waxes.

Absorption band located at ~1730 cm^{-1} corresponds to (C=O) symmetric stretching from carboxylic or ester groups of polygalacturonic acid from pectin with a small contribution of the acetyl groups from uronic esters attached to hemicelluloses and of the conjugate carbonyl groups of hydroxycinnamic acids from lignin (Chambre and Dochia, 2018., 2020.; Chambre et al., 2019; Donatelli et al., 2017). The intense absorption band located at 1732 cm^{-1} in the jute fibers spectrum confirms the higher content of pectin.

The peak recorded at ~1505 cm cm^{-1} and ~ 1595 cm^{-1} are specific to carbon double bond (C=C) and the vibrations of polyphenolic groups of lignin (El-Abbassi et al., 2020; Wang et al., 2019). Another specific band for lignin can be observed at ~1248 cm^{-1} and corresponds to C-O, C-C, C=O, and G ring stretching vibrations (Abdel-Halim et al., 2008; Donatelli et al., 2017; El-Abbassi et al., 2020).

The peak centered at ~1424 cm^{-1} is assigned to asymmetric (CH_2) bending vibration in cellulose (Choe et al., 2018; Fan et al., 2012; Ouajai and Shanks, 2005; Rémy Legrand et al., 2020). This band is also known as the "crystallinity band", and the decrease in the intensity of this band reflects a decrease in the crystallinity degree of the samples (Ciolacu et al., 2011; Fan et al., 2012; Ouajai and Shanks, 2005).

The peak recorded at ~1367 cm^{-1} can be assigned to in-plane bending of (C-OH) groups from cellulose (El-Abbassi et al., 2020; Poletto et al., 2014; Rémy Legrand et al., 2020) and that one of ~1317 cm^{-1} at bending vibration of (CH_2) and (C-OH) groups from cellulose (Poletto et al., 2014; Rémy Legrand et al., 2020). The absorbance of the 1367 cm^{-1} peak is useful to determine the index of crystallinity of the fibers samples. Finally, the small peak located at ~897 cm^{-1} can be assigned to the stretching vibration of β-(1→4) glycosidic linkage of (C-O) groups in cellulose (Ciolacu et al., 2011; Poletto et al., 2014; Rémy Legrand et al., 2020). This band is also known as an "amorphous absorption band" and the intensity of this band increase in the amorphous samples (Ciolacu et al., 2011; Fan et al., 2012; Ouajai and Shanks, 2005).

Infrared crystallinity ratio (LOI, TCI) and Hydrogen Bond Intensity (HBI)

The crystallinity ratio determination of the fibers samples using FTIR spectroscopy is a simple method but it is necessary to underline that this method gives only relative values, because the fibers spectrum always contains contributions from both crystalline and amorphous regions (Fan et al., 2012). To calculate the empirical crystallinity index of cellulose, O'Connor (O'Connor et al., 1958) proposed in 1958 the *Lateral Order Index* (*LOI*) as a ratio between the absorbance values of the bands from 1420 cm^{-1} and 893 cm^{-1} ($LOI = A_{1420} / A_{893}$). These bands are sensitive to the amount of crystalline versus amorphous structure in cellulose and enlargement of these bands reflects a more disordered structure. A few years later, for the same purpose, Nelson and O'Connor (Nelson and O'Connor, 1964a, b) introduced the *Total Crystallinity Index* (*TCI*) as a ratio between the absorbance values of the bands at 1370 cm^{-1} and 2900 cm^{-1} ($TCI = A_{1370} / A_{2900}$) to evaluate the infrared crystallinity index.

According to Polleto et al. (Poletto et al., 2014), *TCI* is proportional to the crystallinity degree of cellulose while *LOI* is correlated to the overall degree of order in cellulose.

Taking into consideration the chain mobility of cellulose and bond distance between chains, the *Hydrogen Bond Intensity* (*HBI*) of cellulose is correlated to the degree of crystallinity which reflects the intermolecular regularity, as well as to the amount of bound water (Poletto et al., 2014). From the vector normalized and baseline corrected FT-IR spectra of the investigated bast fibres (triplicate) the absorbance values of the ~1424 cm^{-1}, 894 cm^{-1}, 1367 cm$^{-1,}$ and 2920 cm^{-1} band were determined and the *LOI* and *TCI* were calculated with (Eq1.) and (Eq2.). The ratio between the absorbance bands at 3400 and 1320 cm$^{−1}$ was used to study the *HBI* of the fibers. The obtained results are shown in Table 3.

Table 3. Infrared crystallinity ratio and hydrogen bond intensity for the investigated bast fibres

Fibres	Infrared crystallinity ratio		Hydrogen bond intensity (*HBI*)
	(LOI)	*(TCI)*	
Flax	1.189±0.093	0.594±0.102	1.084±0.152
Jute	1.833±0.158	0.781±0.088	2.250±0.153
Hemp	2.158±0.108	0.648±0.060	1.946±0.046

Table 3 shows that for the jute and hemp fibers the infrared crystallinity ratio values *LOI* are higher than those obtained for the flax fibers, thus indicating a higher degree of crystallinity and a more ordered cellulose structure. The presence of non-cellulosic attendants (i.e. waxes, hemicelluloses) influences the overall crystallinity of the material. Thus, the high content of amorphous compounds like waxes and extractable substances in flax fibers led to the value of 0.594 for *TCI*, being in accordance with the data reported in the literature by (Kovačević et al., 2012). In addition, the low value for *LOI* (1.189) indicates that the cellulose in the investigated flax fibers is composed of more amorphous regions than in the other two bast fibers.

For hemp fibers, the highest value of *LOI* (2.158) suggests that the cellulose polymer presents more laterally ordered macromolecular chains that allow more intermolecular hydrogen bonds. Comparable values for *LOI* of hemp fibers were reported in the literature by (Ouajai and Shanks, 2005).

According to Poletto et al. (Poletto et al., 2014), a higher cellulose crystallinity of the fibers usually leads to high *HBI* values. This behaviour was observed also for the tree analysed bast fibers. Thus, hemp samples that showed the highest degrees of crystallinity *LOI* also had a higher value for *HBI* (1.946). It should be noted that the *HBI* value reflects both the hydrogen bonds specific to the cellulosic polymer and the hydrogen bonds characteristic of non-cellulosic components. According to Table 1, the jute fibers had the highest content of lignin, which may form intramolecular hydrogen bonds between neighbour phenolic groups. Thus can be explained the highest value obtained for *HBI* (2.250) for the jute fibers even if it does not show the highest overall degree of order in cellulose (*LOI* = 1.833).

CONCLUSIONS

The characterization of jute, hemp, and flax raw fibers by infrared evaluation of crystallinity ratio (*Total Crystallinity Index* and *Lateral Order Index*) and *Hydrogen Bond Intensity* was done.

The results showed that cellulose from jute fibers has a higher degree of crystallinity (*TCI*) while that of hemp fibers has a higher *LOI* value due to a more ordered structure, with more cellulose chains in a highly organized form. In the flax fibers, the native cellulose chains are composed of a larger number of amorphous domains.

The *TCI* obtained values showed that are strongly influenced by the non-cellulosic attendants content such as waxes from raw fibers while the *HBI* values are influenced by the lignin content.

ACKNOWLEDGEMENTS

This work was supported by a grant of the Romanian National Authority for Scientific Research and Innovation, CNCS-UEFISCDI, project number PN-II-RU-TE-2014-4-1370, and „Centru de Cercetare în Științe Tehnice și Naturale-CESTN" co-funded by European Union through European Regional Development Fund Structural Operational Program "Increasing of Economic Competitiveness" Priority axis 2. Operation 2.2.1. POSCCE Nr. 621/2014 POSCCE.

REFERENCES

Abdel-Halim, E.S., Fahmy, H.M., Fouda, M., 2008. Bioscouring of linen fabric in comparison with conventional chemical treatment. Carbohydrate Polymers 74, 707-711.

Bakri, M.K., Jayamani, E., 2016. Comparative Study Of Functional Groups In Natural Fibers: Fourier Transform Infrared Analysis (FTIR), pp 167-174.

Chambre, D.R., Dochia, M., 2018. Characterization of alkaline and enzimatically treated hemp fibers by FT-IR ATR spectroscopy. Scien. Tech. Bull-Chem. Food Sci. Eng. 15,, 18-22.

Chambre, D.R., Dochia, M., 2020. Pectin quantification from cellulosic/lignocellulosic raw materials by FT-IR ATR analysis. . Scien. Tech. Bull-Chem. Food Sci. Eng. 17 20-25.

Chambre, D.R., Dochia, M., Gavrilas, S., 2019. TG/DTG analysis of an eco-friendly scoured fabric. Revue Roumaine de Chimie 64, 453-460.

Choe, E.K., Lee, M., Park, K.S., Chung, C., 2018. Characterization of cotton fabric scouring by Fourier transform-infrared attenuated total reflectance spectroscopy, gas chromatography-mass spectrometry and water absorption measurements. Textile Research Journal 89, 2305-2315.

Ciolacu, D., Ciolacu, F., Popa, V., 2011. Amorphous cellulose - Structure and characterization. Cellulose Chemistry and Technology 45, 13-21.

Dai, D., Fan, M., 2010. Characteristic and Performance of Elementary Hemp Fibre. Materials Sciences and Applications 01, 336-342.

Dochia, M., Chambre, D., Gavrilaş, S., Moisă, C., 2018. Characterization of the complexing agents' influence on bioscouring cotton fabrics by FT-IR and TG/DTG/DTA analysis. Journal of Thermal Analysis and Calorimetry 132, 1489-1498.

Donatelli, A., Cuna, D., Tagliente, M., Protopapa, M., Mevoli, A., Aversa, P., Blasi, C., Capodieci, L., Luprano, V.A.M., 2017. Effect of treatments on the aging behaviour of hemp fibres for building construction in the Mediterranean Area. Journal of Building Engineering 11, 37-471.

El-Abbassi, F.E., Assarar, M., Ayad, R., Bourmaud, A., Baley, C., 2020. A review on alfa fibre (Stipa tenacissima L.): From the plant architecture to the reinforcement of polymer composites. Composites Part A: Applied Science and Manufacturing 128, 105677.

Fan, M., Dai, D., Huang, B., 2012. 3 Fourier Transform Infrared Spectroscopy for Natural Fibres. Fourier Transform-Materials Analysis.

Kovačević, Z., Vukušić, S.B., Zimniewska, M., 2012. Comparison of Spanish broom (Spartium junceum L.) and flax (Linum usitatissimum) fibre. Textile Research Journal 82, 1786-1798.

Manaia, J.P., Manaia, A.T., Rodriges, L., 2019. Industrial Hemp Fibers: An Overview. Fibers 7.

Mustata, F., Tudorachi, N., Mustata, A., Mustata, F., 2015. Physical and thermal characterization of some cellulose fabrics as reinforced materials for composite. Journal of Thermal Analysis and Calorimetry 120.

Nelson, M.L., O'Connor, R.T., 1964a. Relation of certain infrared bands to cellulose crystallinity and crystal lattice type. Part II. A new infrared ratio for estimation of crystallinity in celluloses I and II. Journal of Applied Polymer Science 8, 1325-1341.

Nelson, M.L., O'Connor, R.T., 1964b. Relation of certain infrared bands to cellulose crystallinity and crystal latticed type. Part I. Spectra of lattice types I, II, III and of amorphous cellulose. Journal of Applied Polymer Science 8, 1311-1324.

O'Connor, R.T., DuPré, E.F., Mitcham, D., 1958. Applications of Infrared Absorption Spectroscopy to Investigations of Cotton and Modified Cottons: Part I: Physical and Crystalline Modifications and Oxidation. Textile Research Journal 28, 382-392.

Ouajai, S., Shanks, R.A., 2005. Composition, structure and thermal degradation of hemp cellulose after chemical treatments. Polymer Degradation and Stability 89, 327-335.

Poletto, M., Ornaghi, H.L., Zattera, A.J., 2014. Native Cellulose: Structure, Characterization and Thermal Properties. Materials (Basel) 7, 6105-6119.

Rémy Legrand, N.B., Lucien, M.a., Pierre, O., Ebanda, F., Anicet, N., Jean, A., 2020. Physico-Chemical and Thermal Characterization of a Lignocellulosic Fiber, Extracted from the Bast of Cola lepidota Stem. Journal of Minerals and Materials Characterization and Engineering 08, 377-392.

Shahzad, A., 2012. Hemp fiber and its composites - A review. Journal of Composite Materials - J COMPOS MATER 46, 973-986.

Shamolina, I.I., Bochek, A.M., Zabivalova, N.M., Medvedeva, D.A., Grishanov, S., 2003. An investigation of structural changes in short flax fibres in chemical treatment. Fibres and Textiles in Eastern Europe 11, 33-36.

Summerscales, J., Dissanayake, N.P.J., Virk, A.S., Hall, W., 2010. A review of bast fibres and their composites. Part 1 – Fibres as reinforcements. Composites Part A: Applied Science and Manufacturing 41, 1329-1335.

Väisänen, T., Batello, P., Lappalainen, R., Tomppo, L., 2018. Modification of hemp fibers (Cannabis Sativa L.) for composite applications. Industrial Crops and Products 111, 422-429.

Wang, H., Memon, H., Hassan, E., Miah, M., Arshad, M., 2019. Effect of Jute Fiber Modification on Mechanical Properties of Jute Fiber Composite. Materials 12, 1226.

ISSN 1582-1021
e-ISSN 2668-4764
Edited by “AUREL VLAICU” University
Arad, Romania